Predominant air-sea states during coastal marine heatwaves

Robert W. Schlegel[a,*], Eric C. J. Oliver[b,c,d], Sarah Kirkpatrick[e], Andries Kruger[f,g], Albertus J. Smit[a]

[a] *Department of Biodiversity and Conservation Biology, University of the Western Cape, Private Bag X17, Bellville 7535, South Africa*
[b] *ARC Centre of Excellence for Climate System Science, Australia*
[c] *Institute for Marine and Antarctic Studies, University of Tasmania, Hobart, Australia*
[d] *Department of Oceanography, Dalhousie University, Halifax, Nova Scotia, Canada*
[e] *UWA Oceans Institute and School of Plant Biology, The University of Western Australia, Crawley, 6009 Western Australia, Australia*
[f] *Climate Service, South African Weather Service, Pretoria, South Africa*
[g] *Department of Geography, Geoinformatics and Meteorology, Faculty of Natural and Agricultural Sciences, University of Pretoria, South Africa*

Abstract

As the mean temperatures of the worlds oceans increase, it is predicted that marine heatwaves (MHWs) will occur more frequently and with increased severity however, it is hypothesised that more proximate variables may be responsible for these extreme events. An improved understanding of the mechanisms driving MHWs may allow us to better forecast their occurrence at specific localities. To this end we have utilized atmospheric (ERA-Interim) and oceanic (BRAN) reanalysis data to examine the air-sea state around southern Africa during coastal (<400 m from the low water mark; measured *in situ*) MHWs. Self-organising maps (SOMs) were used to cluster the mean air-sea states during MHWs into 1 of 9 types to determine the predominant patterns. It was found that warm water forced onto the coast via anomalous ocean circulation was the predominant oceanographic pattern during most MHWs. A range of distinct air temperature and wind patterns were found with warm air temperatures over the continent and strong north-westerly winds featuring most prominently during MHWs. It may therefore be possible to forecast the occurrence of MHWs when such air and sea states are projected to occur simultaneously. The lack of any strong air-sea patterns during roughly one third of the MHWs implies that sub-meso-scale activity may have been responsible for them and that finer scale observations may be necessary to deduce their physical drivers. These findings motivate for the implementation of local scale real-time *in situ* monitoring of at risk coastal locations in conjunction with the development of a forecasting and disaster prevention system.

Keywords: extreme events, coastal, atmosphere, ocean, reanalysis data, *in situ* data, climate change

1. Introduction

The anthropogenically forced warming of air, land, and sea have been widely publicized over the last several decades (e.g. Manabe and Wetherald, 1967; Sawyer, 1972; Hansen et al., 1981; Cox et al., 2000; Rosenzweig et al., 2008). Investigations into the negative impacts this warming may have on

*Corresponding author
Email address: 3503570@myuwc.ac.za (Robert W. Schlegel)

ecosystems ranges in focus from long term trends (e.g. Scavia et al., 2002; Walther et al., 2002; Burrows et al., 2011) to shifting states (e.g. Travis, 2003; Grebmeier, 2006; Blamey et al., 2015) to extreme individual events (e.g. Easterling et al., 2000; Barrett et al., 2008; Wernberg et al., 2012). Whereas long term temperature trends are projected to have a negative impact on many of earth's systems (Stocker et al., 2013), and the shifts in thermal states brought about by these long term trends are projected to cause irreversible species loss (Thomas et al., 2004), extreme events pose a more immediate threat to ecosystems (e.g. Jolly et al., 2005; Denny et al., 2009; Hufkens et al., 2012). Extreme thermal events have been given a range of labels but are broadly divided into two categories: cold-spells (e.g. Gunter, 1941; Lirman et al., 2011; Boucek et al., 2016) and heatwaves (e.g. GORDON et al., 1988; Stott et al., 2004; Perkins-Kirkpatrick et al., 2016). We chose here to focus on heatwaves that occur in the sea, classified as 'marine heatwaves' (MHWs).

Several large MHWs, and their ecological impacts, have been well documented. The first of which being the 2003 Mediterranean MHW that negatively impacted as much as 80% of the Gorgonian fan colonies (Garrabou et al., 2009). The 2011 Western Australia MHW is now known to have caused a permanent 100 km range contraction of the ecosystem forming kelp species *Ecklonia radiata* in favour of the tropicalisation of reef fishes and seaweed turfs (Wernberg et al., 2016). The damage caused by MHWs is not confined to demersal organisms or coastal ecosystems as demonstrated by a MHW in the North West Atlantic Ocean in 2012 that impacted multiple commercial fisheries (Mills et al., 2013). When extreme enough, such as "the Blob" that persisted in the North West Pacific Ocean from 2014 to 2016, a MHW may even negatively impact marine mammals and seabirds (Cavole et al., 2016). Analysis of *in situ* coastal seawater temperature time series from South Africa has shown that MHWs of comparable magnitude to those highlighted here have occurred (Schlegel et al., 2017) however, it is not known what damage these events may have caused as little long-term ecological sampling is carried out in the locations of these events.

It is possible to directly compare MHWs occurring anywhere on the globe during any time of year because of a definition developed by Hobday et al. (2016), which was accompanied by the development of a statistical methodology for their calculation. Whereas the metrics created for the measurement of MHWs allowed for the comparison of events, they did not directly reveal what may be causing said events. Beyond common measurements, it is necessary to identify the possible physical drivers of MHWs so as to be able to compare similar 'types' of events and to be able to move towards a system of prediction.

It has been assumed that MHWs should either be caused by oceanic forcing, atmospheric forcing, or a combination of the two however, the scale at which this forcing must occur in order to drive MHWs has yet to be determined. Recent research into the development of a mechanistic understanding between local- *vs.* meso-scale influences on the formation of coastal MHWs has revealed that meso-scale oceanic forcing from offshore onto the nearshore (<400 m from the coast) is far less responsible for the formation of MHWs than hypothesized (Schlegel et al., 2017). It is therefore necessary to consider additional mechanisms that may be responsible for these events. For example, the 2011 Western

Australia MHW (Pearce and Feng, 2013) was caused by the aseasonal transport of warm water onto the coast due to a surge of the Leeuwin Current (Feng et al., 2013; Benthuysen et al., 2014). Conversely, Garrabou et al. (2009) were able to show that atmospheric forcing played a clear role in formation of the 2003 Mediterranean MHW. While more complex, Chen et al. (2015) also showed that air-sea heat flux could be attributed as the main forcing variable in the 2012 Atlantic MHW. "The Blob" however appears to have occurred due to the lack of advection of heat from surface waters into the atmosphere due to anomalously high sea level pressure (Bond et al., 2015). Outside of these few examples for these well documented events there has been little progress in developing a global understanding of the forcing of MHWs more broadly.

In order to develop a methodology that could investigate the potential air and/ or sea forcing of multiple coastal MHWs simultaneously, an index of mean synoptic air-sea states during the occurrence of these events was created. These states were then clustered with the use of a self-organising map (SOM). The aim of the clustering of the synoptic air-sea states was to visualise patterns in the air and/ or sea that occur during MHWs at coastal sites. We hypothesized that i) air and sea mesoscale patterns would be revealed through clustering; ii) these patterns would be more distinct in the sea than in the air; and iii) the air-sea states would aid in the development of a broader mechanistic understanding of the physical drivers of coastal MHWs.

2. Methods

2.1. Study region

The *ca.* 3,100 km long South African coastline provides a natural laboratory for investigations into the forcing of nearshore phenomena as it may be divided into three distinct sections, allowing for a range of meso-scale oceanographic influences to be considered within the same research framework (Figure 1). The entire west coast section of the country is distinct from the other two as it is bordered by the Benguela Current, which forms an Eastern Boundary Upwelling System (EBUS) (Hutchings et al., 2009). Conversely, the east coast section is dominated by the Agulhas Current (Lünning, 1990), a poleward flowing body of warm water. The south coast section is also bordered by the Agulhas current but differs from the east coast section in that it experiences both shear-forced and wind-driven upwelling (Lutjeharms et al., 2000) in addition to having significantly more thermal variability than either of the other two sections (Schlegel et al., 2017). The range of temperatures experienced along all three sections are large and the gradient of increasing temperature as one moves from the border of Namibia (site 1) to the border of Mozambique (site 26) is nearly linear. For a more detailed description of these sections see Smit et al. (2013). The extent of the study area used here was 10°E to 40°E and 25°S to 40°S.

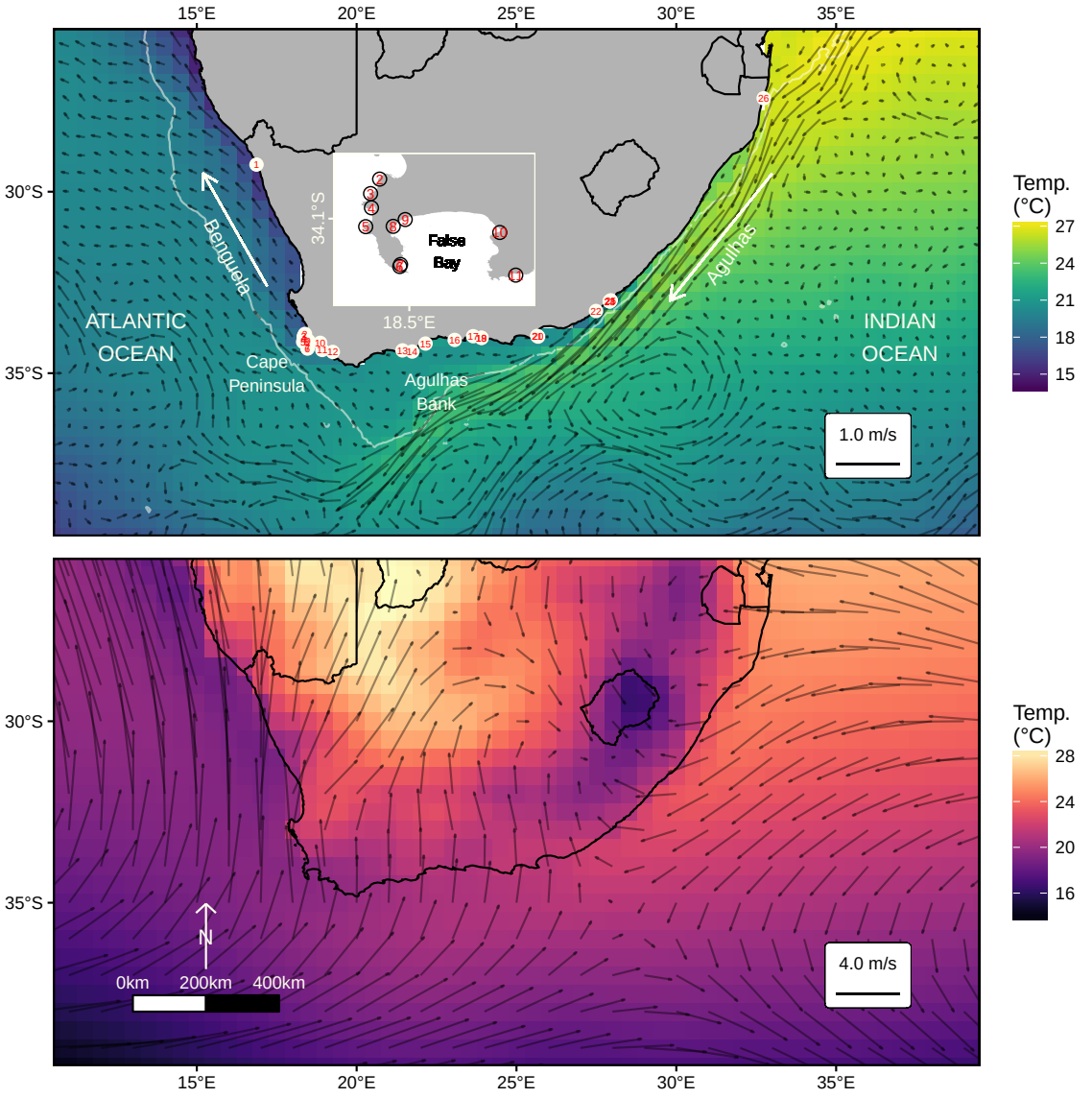

Figure 1: A two panel map of southern Africa. The top panel shows the mean January 1st sea surface temperature (SST) and surface currents from BRAN data as well as the locations refereed to in the text. The locations of *in situ* collection are shown with red numerals over white circles. An inset map of the Cape Peninsula/ False Bay area is shown where site labels are obscured due to overplotting of symbols. The bottom panel shows the mean January 1st surface air temperature and winds from ERA-Interim data as well as a North arrow and scale bar. Note that the temperature and vector scales differ between the two panels.

2.2. Data

2.2.1. In situ *data*

The *in situ* coastal seawater temperature data used in this study were acquired from the South African Coastal Temperature Network (SACTN, https://github.com/ajsmit/SACTN, https://robert-schlegel.shinyapps.io/SACTN/). These SACTN data are contributed by seven different organizations and are collected *in situ* with a mixture of hand-held alcohol & mercury thermometers as well as digital underwater temperature recorders (UTRs). This data set currently consists of 135 daily time series, with a mean duration of 19.7 years. Therefore many of the time series in this dataset are shorter than the 30 year minimum proscribed for the characterisation of marine heatwaves (MHWs, see 'Marine heatwaves' section below) (Hobday et al., 2016). It is however deemed necessary to use these data when investigating extreme events in the nearshore (<400 m from the low tide mark) as satellite derived sea surface temperature (SST) values along the coast have been shown to display large biases (Smit et al., 2013) or capture minimum and maximum temperatures poorly (Smale and Wernberg, 2009; Castillo and Lima, 2010). Whereas a 30+ year period is ideal for determining a climatology, ten years may serve as an acceptable bottom limit (Schlegel et al., 2017). Following on from the methodology laid out in Schlegel et al. (2017) time series with more than 10% missing data were also excluded from this research. Accounting for these 10 year length and 10% missing data constraints, the total number of *in situ* time series used in this study was reduced to 26, with a mean length of 22.3 years. Table 3 shows the metadata for the SACTN time series used in this study (RWS: I don't think a supplemental section should be given here, rather host everything on GitHub).

2.2.2. Reanalysis data

To visualise a synoptic view of the air and sea states during coastal marine heatwaves (see sections 'Marine heatwaves' and 'Air-sea state' below) it was necessary to use reanalysis data to provide air and sea temperatures with wind and current vectors in a single product.

The 1/10°B̃luelink ReANalysis (BRAN2016, hereafter referred to as BRAN) product was chosen for sea surface temperature (SST) and surface current data. This modelled product relies on the assimilation of an array of data collected *in situ* and remotely. BRAN is available for download via XML and is a product of the CSIRO (https://www.csiro.au/). (RWS: Should more be said about BRAN? Should the CSIRO web-link be included?)

The surface air temperature (2 m) and winds (10 m) were determined with the use of the ERA-Interim reanalysis product and were downloaded at a resolution of 1/2°. This comprehensive global atmospheric model assimilates a wide range of data (Dee et al., 2011). ERA-Interim is produced by the European Centre for Medium-Range Weather Forecasts (ECMWF, http://www.ecmwf.int/) and is available for download through a web-based user interface.

To ensure even sampling of the synoptic air and sea states the BRAN data were averaged on a 1/2°g̃rid to match the resolution of the ERA-Interim data. Both datasets were then trimmed to contain the same longitude and latitude extents as the study area. All variables were then coerced into the

same dataframe format for consistent analysis. The BRAN reanalysis product at the writing of this paper was available from January 1st, 1994 to August 31st, 2016. This is less than the range of data currently available for ERA-Interim at January 1st, 1979 to December 31st, 2016. All dates occurring outside of those in the BRAN product were excluded. The analysis period for the climatologies for the BRAN and ERA-Interim data used in this research was therefore set as January 1st, 1979 to December 31st, 2016.

2.3. Marine heatwaves

We use the definition for a MHW given by Hobday et al. (2016) as "a prolonged discrete anomalously warm water event that can be described by its duration, intensity, rate of evolution, and spatial extent" as well as the methodology laid out in Hobday et al. (2016) for the analysis of MHWs in this research. The algorithm developed by Hobday et al. (2016) isolates MHWs by finding the days in which the temperature of a given locality exceeds the 90th percentile of temperatures found there on that given day, based on an 11-day moving window, for a certain number of days. Perkins and Alexander (2013) concluded that the minimum duration for the analysis of atmospheric heatwaves was 3 days whereas Hobday et al. (2016) found that a minimum length of 5 days allowed for more uniform global results for the detection of heatwaves in the ocean. It was also determined that any MHW that had 'breaks' below the 90th percentile threshold lasting $\leq$2 days followed by subsequent days above the threshold were considered as one continuous event (Hobday et al., 2016). Previous work by Schlegel et al. (2017) showed that the inclusion of these short 5 day MHWs may lead to spurious connections between events found across different datasets. Therefore we have limited the inclusion of MHWs to those with a duration in the top 10th percentile of all events detected along the coast and that occurred within the range of dates for the reanalysis data. Thus, from the 976 total MHWs detected in the *in situ* dataset, only 98 were taken.

In order to calculate a MHW it is necessary to supply a climatology against which daily values may be compared. It is proscribed in Hobday et al. (2016) that this period be at least 30 years. Because 20 of the 26 time series used here are below this threshold we have opted to use the first and last complete years of data for each individual time series as the boundaries of the climatological period. Using fewer than 30 years of data to determine a climatology prevents the accurate inclusion of any decadal scale variability (Schlegel and Smit, 2016) however, by using at least 10 years of data we are able to establish a baseline climatology to calculate MHWs (Schlegel et al., 2017). By calculating MHWs against the daily climatologies from their time series in this way the amount they differ from their localities may be quantified and compared across time and space. Meaning that this allows researchers to examine events from different variability regimes (i.e. regions of the world) and compare them with a consistent set of MHW metrics. The definitions for the metrics that will be focused on in this paper may be found in Table 1.

The MHWs in the SACTN dataset were calculated via the R package 'RmarineHeatWaves', which may be downloaded via CRAN (https://cran.r-project.org/web/packages/RmarineHeatWaves/index.html), with the developmental version available on GitHub (https://github.com/ajsmit/RmarineHeatWaves).

Table 1: The descriptions for the metrics of MHWs as proposed by Hobday et al. (2016) and adapted from Schlegel et al. (2017).

Name [unit]	Definition
Count [no. events per year]	n: number of MHWs per year
Duration [days]	D: Consecutive period of time that temperature exceeds the threshold
Maximum intensity [°C]	i_{max}: highest temperature anomaly value during the MHW
Mean intensity [°C]	i_{mean}: mean temperature anomaly during the MHW
Cumulative intensity [°C·days]	i_{cum}: sum of daily intensity anomalies over the duration of the event
Onset rate [°C/day]	r_{onset}: daily increase from event onset to maximum intensity
Decline rate [°C/day]	$r_{decline}$: daily decrease from maximum intensity to event end

The original algorithm used in Hobday et al. (2016) is available for use via python and may be found at https://github.com/ecjoliver/marineHeatWaves.

It is necessary to emphasise that MHWs as defined here exist against the daily climatological means of the time series in which they are found and not by exceeding an arbitrarily chosen static threshold. Therefore, one may just as likely find a MHW during winter months as summer months. This is a valuable characteristic of this method of investigation because aseasonal warm winter waters may have deleterious effects on relatively thermophobic species (Wernberg et al., 2011), or aid the recruitment of invasive species (Stachowicz et al., 2002).

2.4. Air-sea states

In order to visualise any possible patterns in the air and sea around southern Africa during a coastal MHW it was necessary to first create daily synoptic images of the air-sea states for all days available in the reanalysis data downloaded for this research. The synoptic sea states consisted of SST and surface currents while the air states showed surface air temperatures and surface winds. For each of the 98 MHWs in this study, the daily synoptic air-sea states during an individual event were averaged together to create one mean air-sea state. For example, if a MHW started on December 1st, 1999, and ended on March 7th, 2000, those 98 daily synoptic air-sea states were averaged to create a single air-sea state that represented the overall pattern that was occurring during that one event. This may be seen in the top row of panels in Figure 2.

The calculation of anomalies required first that a daily climatology be created for the air and sea states. These 366 climatologies were calculated using the same 11-day moving window used to determine the daily climatologies within the *in situ* time series against which the MHWs were calculated. With the average air-sea state known for each calendar day of the year, it was then possible to subtract these daily climatologies from the daily air-sea states during which a MHW was occurring before averaging each individual daily anomaly together to create one mean anomalous air-sea state. An example of the anomalous air-sea states created in this way may be seen in the middle row of Figure 2.

With the calculation of the 366 daily climatologies for the air-sea states it became possible to determine if the air-sea states during the days in which a MHW was occurring differed. Multi-dimensional scaling (MDS) was performed on the 366 daily air-sea climatologies and the 98 mean air-sea states. MDS was used here as it allows for the strength of the influence of categorical variables to be displayed

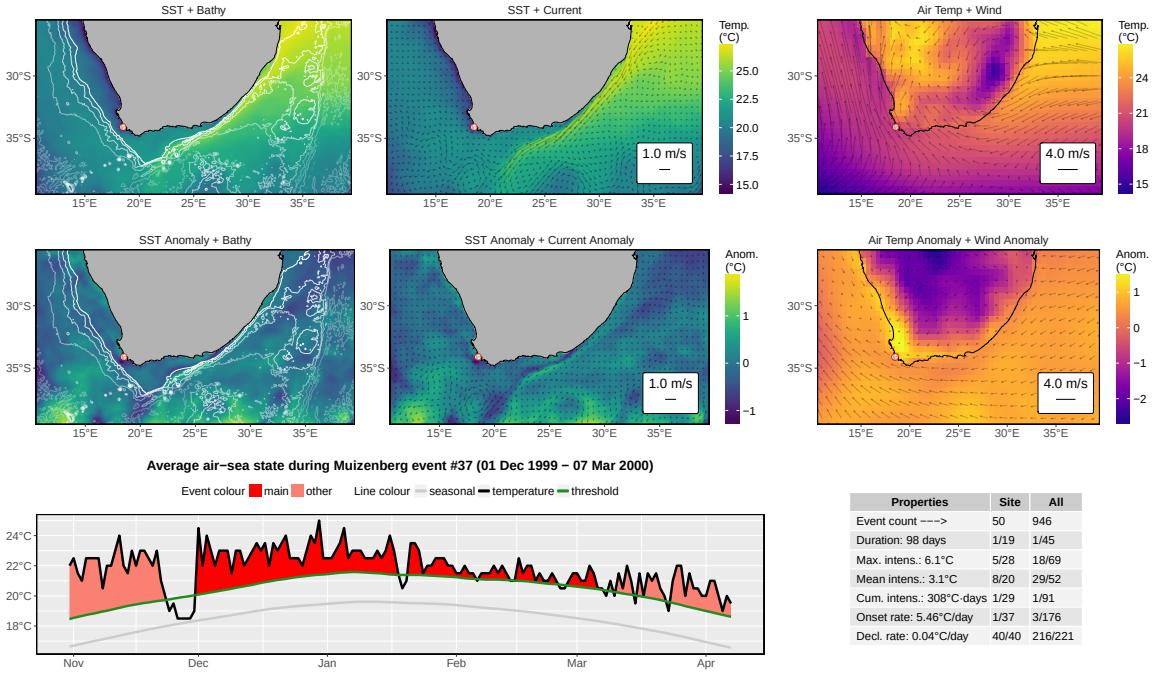

Properties	Site	All
Event count −−−>	50	946
Duration: 98 days	1/19	1/45
Max. intens.: 6.1°C	5/28	18/69
Mean intens.: 3.1°C	8/20	29/52
Cum. intens.: 308°C·days	1/29	1/91
Onset rate: 5.46°C/day	1/37	3/176
Decl. rate: 0.04°C/day	40/40	216/221

Figure 2: Multiple panelled figure showing a range of information on a single coastal marine heatwave (MHW). The location of collection for the *ins situ* coastal seawater temperature time series is shown in each of the top six panels as a white dot with a red outline. The top row of panels shows the mean synoptic air and sea states during the MHW, created by averaging all daily air-sea states during the event. The middle row shows anomalies for the mean air and sea states during the event. The mean anomalies were calculated by first subtracting the daily climatology before then averaging all of the days together. The left hand panel in the bottom row shows the 'shape' of the MHW and the dates during which it occurred. The table in the bottom left corner shows the values for the relevant metrics of the event as explained in Table 1 as well as their ranking against other events at the same site and all of the MHWs detected along the coast. Similar figures for each of the 98 longest MHWs are available here: https://github.com/schrob040/AHW/tree/master/graph/synoptic .

on the resultant bi-plot as vectors. The categorical variables considered when ordinating the daily and mean air-sea states together were the four seasons during which the day or event occurred/ started, as well as if the value represented a daily climatology or an event. To further investigate the possible relationship between the four seasons and the occurrence of MHWs, hierarchical cluster analysis (HCA) was performed on these combined data with a cutoff at four groups, presumably one for each season. This would allow us to determine first if the daily climatologies grouped themselves according to their season, and second to see if the events clustered themselves within the season during which they occurred, or if some other pattern would emerge.

2.5. Self-organizing Map

Several methods of clustering synoptic data have been employed in climate science. Of these K-means clustering is perhaps most often employed (e.g. Corte-Real et al., 1998; Burrough et al., 2001; Kumar et al., 2011), with hierarchical cluster analysis (HCA) less so (e.g. Unal et al., 2003). A newer technique, self-organizing maps (SOMs), has been gaining in popularity in climate studies over the past decade (e.g. Cavazos, 2000; Hewitson and Crane, 2002; Morioka et al., 2010). Here we have used a SOM to cluster the mean air-sea state anomalies for each of the 98 MHWs.

The initialisation of a SOM is similar to more traditional clustering techniques in that a given number of clusters (hereafter refereed to as nodes) are declared by the user before the SOM algorithm randomly assigns each data point into one of said nodes. The SOM then iteratively changes the node for each of the data points until the stress within each node, measured as within group sum of squares (WGSS), is reduced as much as possible (Jain, 2010). Stress here refers to the total variance between data points in each cluster (cite, probably (Jain, 2010)). With large amounts of residual variance meaning the model is fit poorly. SOMs differ from more traditional clustering algorithms in that they also account for the between node stress and endeavour to orient the nodes into the least stressful position possible within a two dimensional space (cite). This allows the user to see not only into which nodes the data points (mean air-sea state anomalies) best belong in, but also what the relationship between the nodes may be (cite). (RWS: Shall more technical details be given here? It may be better to move half of this paragraph up to the previous one.)

Because the SOM algorithm was not able to provide consistent results each time the analysis was run, we opted out of using the default random initialization (RI) for the SOM in favour of principal component initialization (PCI). PCI differs from RI in that it uses the two principal components of the dataset, as determined from a principal component analysis (PCA) to initialize the choice of node centres for the SOM. This allows the SOM model to create the exact same result whenever it is run on the same data. (RWS: Is it necessary to validate the PCA in more detail here?)

Once each event, as represented by its mean air-sea state anomalies, was clustered into a node, a further mean air-sea state anomaly for each node was calculated by taking the average of all of the mean air-sea state anomalies clustered within each node. It was these final mean air-sea state anomalies that were taken as the predominant air-sea states during coastal MHWs.

3. Results

(RWS: This whole subsection should probably go...)

As it is outside of the focus of the research presented here, we will not go into detail on the differences in the results generated by the three aforementioned methods. We will state however that it was the SOMs that best clustered out the data when all methods were visualised in two dimensions via a principal component analysis (PCA) (RWS: Consider moving this to results). In addition to the superior pattern recognition displayed by the SOM method, the orientation of the nodes (clusters) as produced by the SOM is also of use to the interpretation of the results of this work.

3.1. Self-organizing Map

(RWS: Potential some of this should go in the methods.)

The appropriate number of nodes to use in a cluster analysis is well known to be a contentious decision (cite). We have chosen here to use 9 nodes for a number of reasons. The first reason was that SOMs are best run on even grids of data (e.g. 2x3, 3x3, 4x4, etc.) (RWS: cite why even grids are best). Calculating the within group sum of squares (WGSS) value as more nodes were included showed that 4 could be satisfactory, but that at least 6 would be better.

Ultimately we settled on 9 nodes as this allowed for a wider variety of different synoptic air-sea states to be separated out from one another, allowing for a better understanding of the dominant air-sea states that exist during coastal MHWs to be formed.

A final consideration for the validity of the choice of nodes, as proposed in Johnson (2013), is that the nodes must be significantly different from one another. Using an analysis of similarity (p=xxx) we found this to be true for the choice of 9 nodes. (RWS: Move this last sentence to results after re-writing this paragraph)

Due to a lack of consensus in the literature around the best practices for clustering synoptic air-sea states, we decided to compare K-means, HCA and SOM clustering results against one another. Figure 3 shows the results of each clustering technique when each synoptic air-sea state is laid out on a two dimensional plane as determined via a PCA. One may see that the SOM analysis is best able to determine distinct different clusters. Surprisingly HCA appears to produce slightly more distinct clusters than K-means, but both are inferior to the SOM results.

3.2. Air-sea states

(RWS: Merge this with the following section)

The 9 most common air-sea states around southern Africa during coastal MHWs may be seen in Figure 4. The top nine panels show the SST and currents, while the bottom 9 panels show the air temperature and winds. All values shown are anomalies. One may note that the patterns in the wind and air temperature states are more clear and pronounced than the SST and currents.

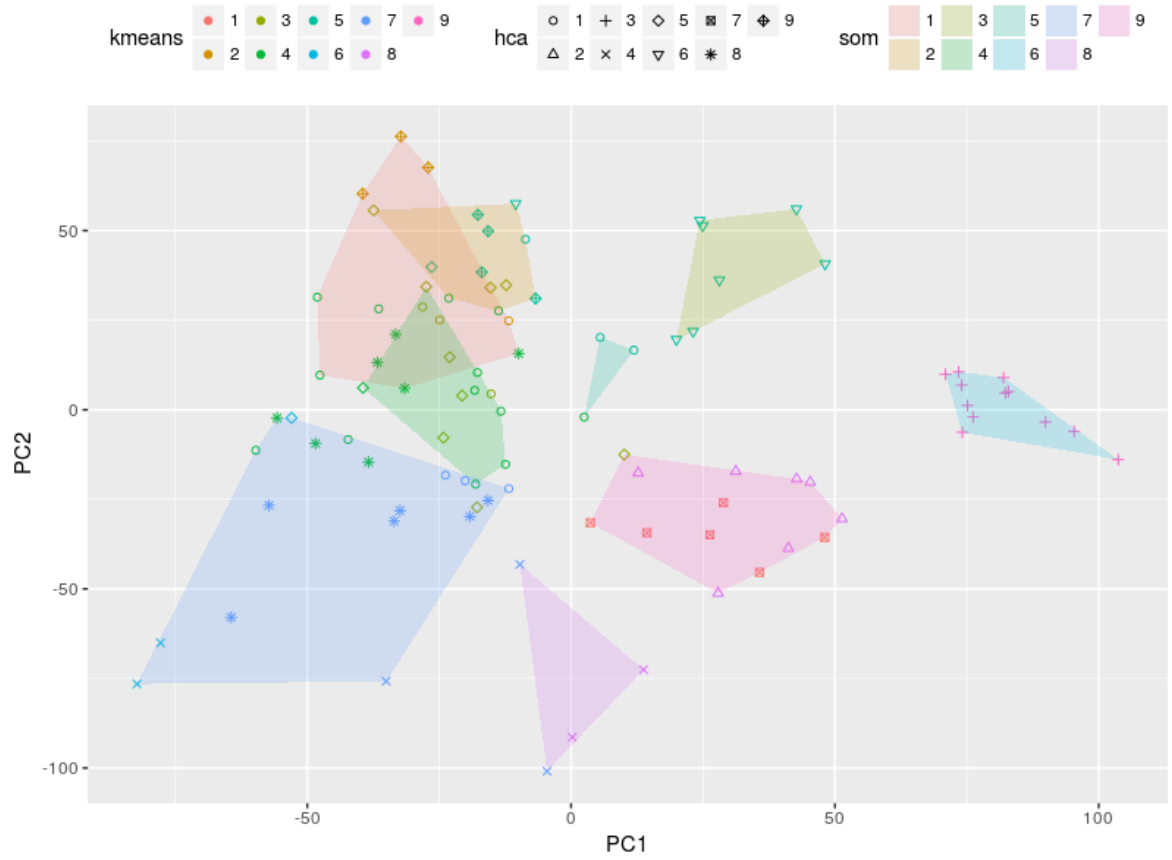

Figure 3: Results for each of three different clustering techniques used to determine the groupings of synoptic air-sea states during coastal MHWs. (RWS: I think I will rather show the results for each technique as separate facets, rather than plotting them together like this.).

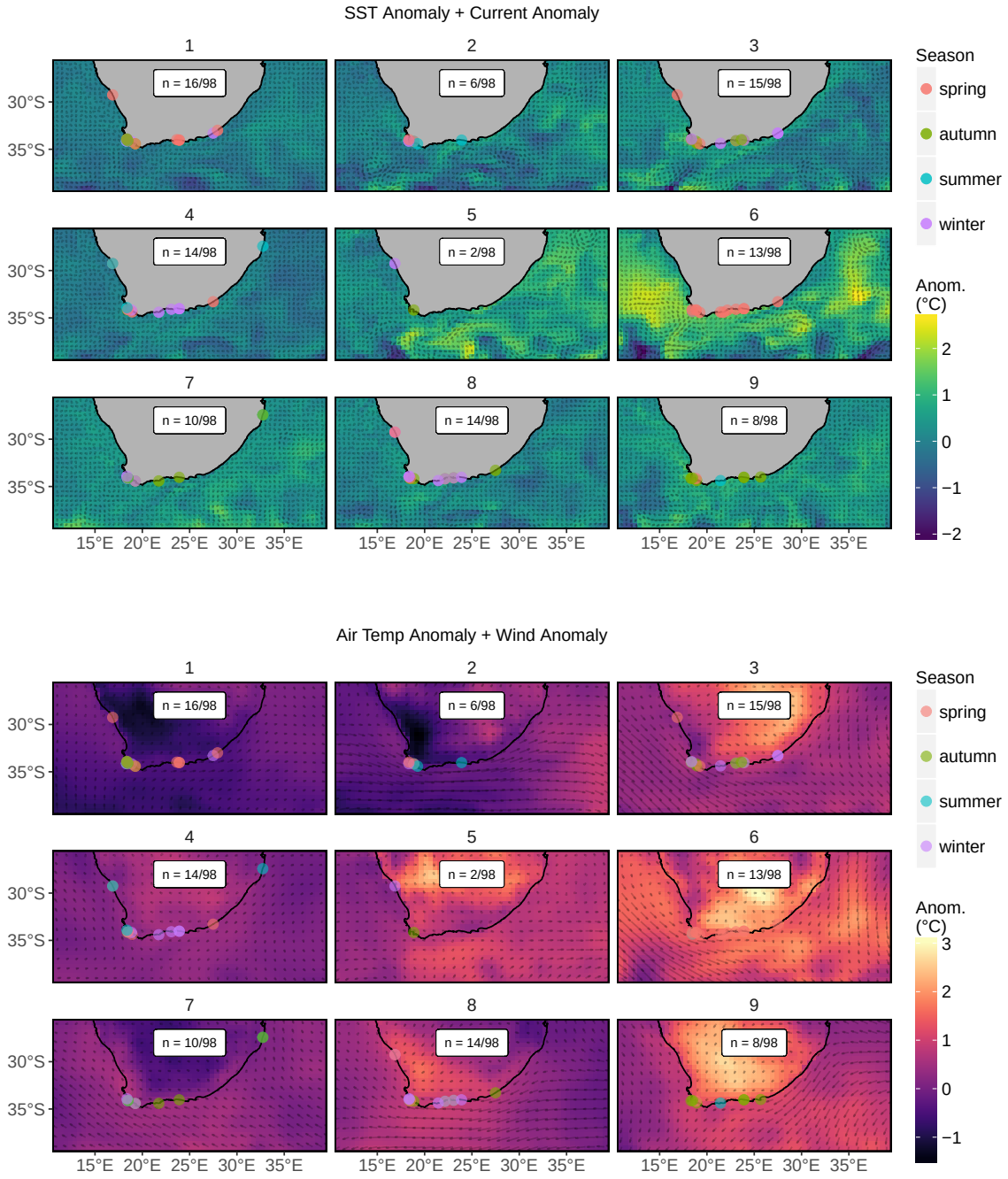

Figure 4: Common air and sea states during coastal marine heatwaves (MHWs). (RWS: I suggest a colourbar that has 0=white, e.g. blue-white-red ditto for air temp below that way we can tell what is cooler than avg and what is warmer than avg. Also improve the vectors for currents.)

3.3. Nodes

(RWS: Describe each node individually, using the subsections they have been split across as guidelines for what to focus on.) (RWS: Consider finding out which pixels are significantly different from the means within the nodes.)

Immediately apparent in the clustering of the data is that node 6 stands out in starkest contrast to the other nodes the most anomalously warm air and sea states as well as having the strongest winds and currents. As one moves from the right hand nodes to the left they become progressively less intense. With less and less of a pattern present. These left hand nodes serve to show that there are still many coastal MHWs that occur without any strong meso-scale pattern on average. Or at least not a pattern that has occurred often enough over the past 30+ years that would afford them their own node. Due to the vast dissimilarity between the 9 nodes, only 2 events were clustered into the central node. Otherwise the clustering of events into nodes was equitable. Also important to note is that a common pattern in many of the nodes, but particularly node 6, is the abnormal retroflection of the Agulhas current onto the Agulhas Bank (Figure 4).

If we look at the events within the nodes via lolliplots (Figure 5) we see that only one of the nodes shows an air-sea state during primarily one large event that was recorded at multiple locations (node 6). Besides node 6 (and 5), the other nodes consist of a medley of multiple independent events that occurred during different years and seasons, and of varying magnitudes, that cluster together due to their similarity. These nodes represent what a more common air-sea state during a coastal MHW may look like.

3.4. Marine heatwaves

When we look at the mean statistics for each node (Table 2) we see that there is a large difference in the mean duration (days) of MHWs clustered therein. Nodes 4 and 5 show the longest mean durations however, the mean duration in node 5 is skewed by having one very long event and only two total events in that node. Nodes 9 and 2 are characterized by having the shortest MHWs. As large cumulative mean intensities are generally a product of lengthy MHWs, it is not surprising to see that Nodes 4 and 5 also have the highest values for this metric as well. Again though node 5 is misrepresented in this regard due to the one large event clustered there. As for the maximum intensity of events within each node, there is less difference between the nodes than for the other two metrics shown. Nodes 2 and 8 however did have events with the lowest maximum intensities (°C) on average.

3.5. Seasonality

When we consider the seasonal distribution of MHWs in each node, we see that except for node 6, there appears to be no consistency in the season during which a certain air-sea pattern may occur. If we were to plot the air-sea states during MHWs against normal days we see in Figure 6 and Figure 7 that the synoptic air-sea states during the 366 daily climatologies are different from almost all of the synoptic air-sea states during coastal MHWs. As one may see from the flat ellipse of blue squares (the daily climatology points), the variance represented in the x axis is seasonality. Indeed, if the dates are

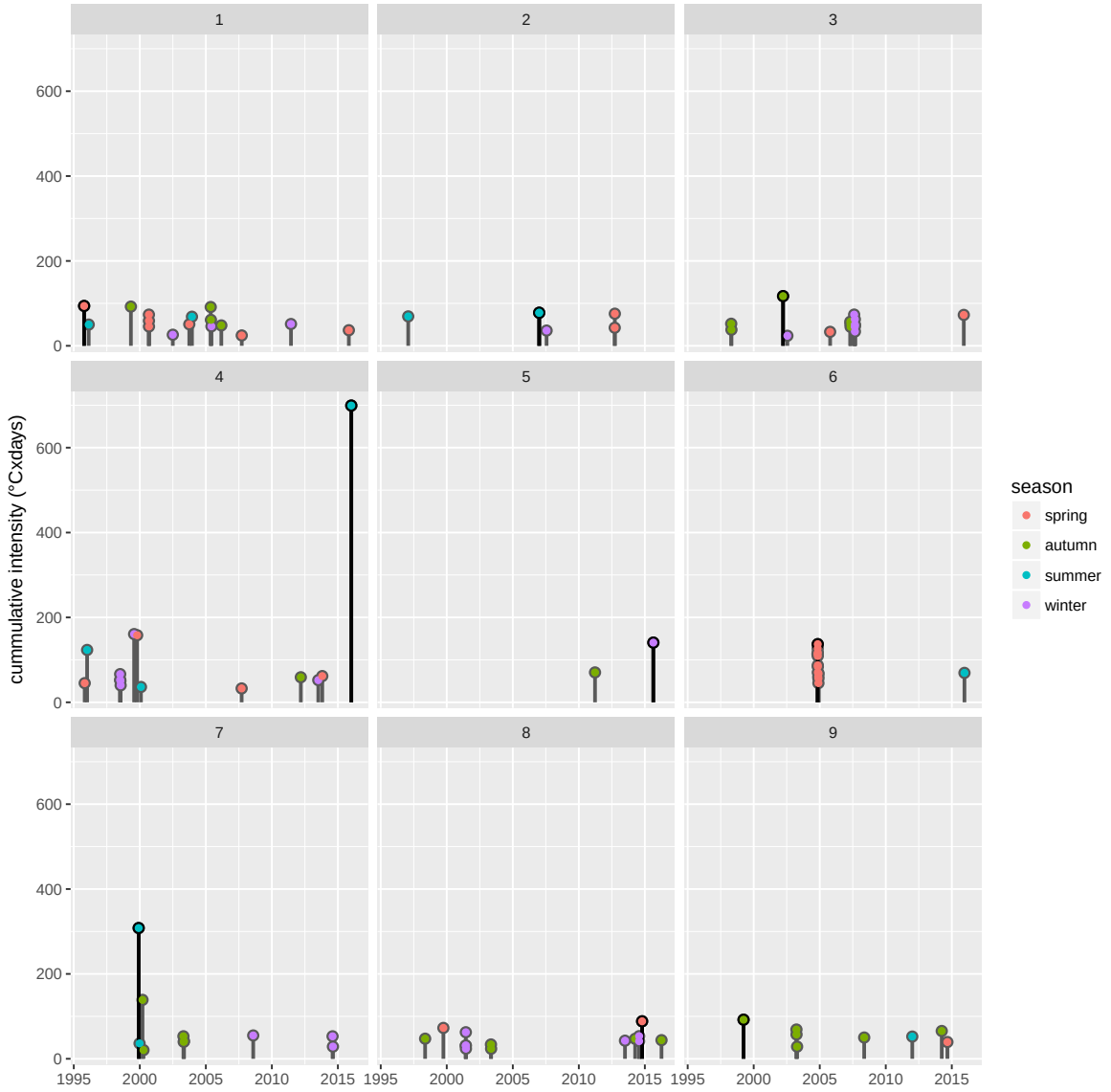

Figure 5: Lolliplot showing the date during which each event began. The height of each lolli shows the cumulative intensity of the event for comparison of the severity of the events.

Table 2: The relevant metrics and statistics for the events found within each node. (RWS: I will add +- standard deviation to the mean columns)

node	count	summer	autumn	winter	spring	west	south	east	duration_mean	int_cum_mean	int_max_mean
1	16	2	4	3	7	7	8	1	22.20	57.48	3.62
2	6	3	0	1	2	2	4	0	18.50	63.26	4.51
3	15	0	6	7	2	4	11	0	23.70	53.47	3.22
4	14	3	1	6	4	3	10	1	43.50	117.09	3.92
5	2	0	1	1	0	1	1	0	42.00	105.59	4.23
6	13	1	0	0	12	0	13	0	31.20	88.12	4.02
7	10	2	5	3	0	1	7	2	30.00	77.53	3.49
8	14	0	5	7	2	4	10	0	20.20	45.99	3.27
9	8	1	6	0	1	1	7	0	17.50	56.85	4.39
ALL	98	12	28	28	30	23	71	4	27.00	71.14	3.72

included in the figure above they are in a nearly contiguous state. With January 1st in the top left edge of the ellipse of blue squares with the dates then moving clockwise. May is roughly in the middle of the top of the ellipse and October in the middle on the bottom. The synoptic states during events appear to be controlled by the variance represented by the y axis. This then must be some sort of variance that is aseasonal. Likely the anomalous characteristics of air and or sea that occur during the events. This shows that whatever those states may be, they are independent from the common air-sea states that occur at any time during the year. Also worth noting is that the daily climatologies for summer and winter do not cluster at all with any of the events (Figure 6). They are almost all clustered with autumn, and a few with spring days.

3.6. Spatiality

As shown in Table 2, there are very few events with durations greater than 15 days that occurred in the east coast section of the study area. Therefore it is difficult to judge any potential relationships between synoptic patterns that may be responsible for events only on the east coast, or between the east coast and other sections of the coastline. Table 2 does show that, with the exception of node 6, there are no nodes that contain only events from one coastal section. 8 of the 9 nodes created by the SOM consist of synoptic air-sea states that were occurring during MHWs separated over large distances and by oceanographically dissimilar features.

3.7. Seasonality

4. Discussion

(RWS: Talk more about how the event days cluster out differently from normal days.)

Schaeffer and Roughan (2017) Sub surface MHWs

Beal et al. (2011) Agulhas leakage likely to increase. This is associated with interglacial periods. Whereas the abatement of leakage is associated with severe glacial periods. This is all due to the north or southward shift of westerly winds over the Atlantic.

(RWS: Change this subsection heading.)

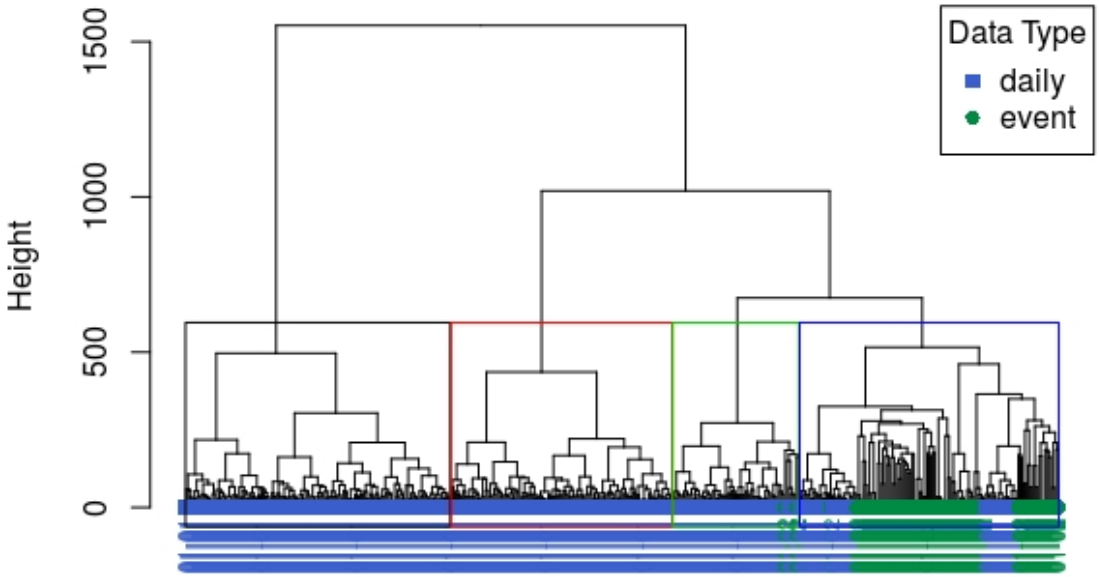

Figure 6: (RWS: I will clean this figure up before submission) Dendrogram showing the distribution of normal daily climatological air-sea states (blue) versus the distribution of mean air-sea states during Marine Heatwaves (MHWs; green). Four clusters are shown as proxies for the four seasons of the year.

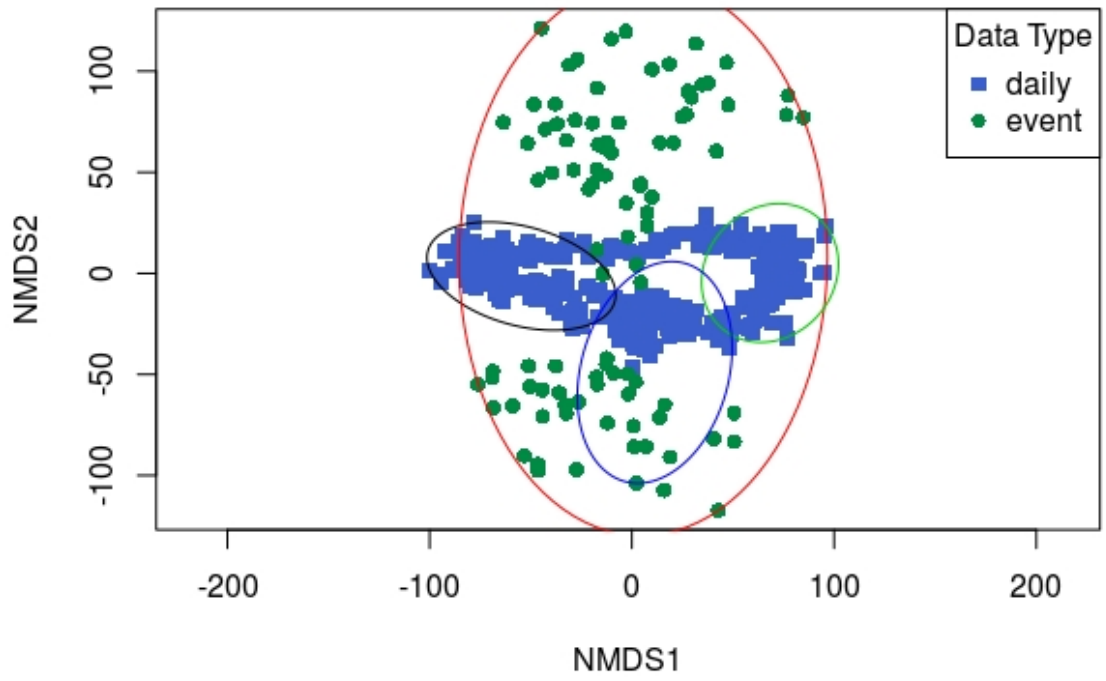

Figure 7: (RWS: I will clean this figure up before submission) Ordiplot showing the distribution of normal daily climatological air-sea states (blue) versus the distribution of mean air-sea states during Marine Heatwaves (MHWs; green). The four clusters from Figure 6 are shown here as ellipsis.

4.1. Anomalous behaviour

Most notable from the clustering of these events has been the Agulhas current retroflecting (RWS: Talk about Agulhas Leakage instead) north onto the Cape Point region, rather than its usual southward retroflection (cite), when coastal MHWs were detected. This is a similar finding to the cause of the Western Australia MHW (Feng et al., 2013; Benthuysen et al., 2014). This onshore push of water is most apparent in panel six of Figure 4 however, panels 7, 3 and 9 also show advection of warm water onto the coast around Cape Point (RWS: Consider moving much of this to the results section.). This shows that the anomalously warm temperatures in the areas where MHWs were detected are due to meso-scale activity, and not any local processes. Nodes 8, 4, 1 and 5 lack the apparent onshore forcing of the Agulhas current. These nodes do not show any apparent anomalous behaviour in the sea. When we look at the atmospheric data we see that there are much clearer patterns at play. This supports the argument that some coastal MHWs may be linked more strongly to atmospheric processes than to meso-scale oceanographic forcing.

4.2. Seasonality

With the exception of node 6, all of the nodes produced by the SOM contain events not only over large periods of time, but during most if not all four seasons of the year. This means that the meso-scale drivers of MHWs are truly aseasonal. Indeed, as we may see in Figure 7, not only do events occurring during a particular season not relate to the air-sea states during that season, they do not relate to air-sea states during any time of the year. The only small exception to this finding being that some small similarities may be noted during some days in spring and several more during autumn. This implies that whereas air-sea states during events depart from anything seen throughout a normal year, they most closely resemble air-sea states during the tumultuous transitional seasons of spring and Autumn (cite?). (RWS: Calculate the difference in variance between the seasons.)

Also of interest in this study was during which season do MHWs in excess of 15 days tend to occur. We found, to some surprise, that only a small portion (Table 2) of MHWs occurred during summer months. This implies that the phenomena that may be driving these long MHWs occur more often during the cooler months of the year. This may mean that summer months around southern Africa are more stable than at other times of the year, or that the processes that drive long MHWs are linked to the transitioning of warmer temperatures to cooler temperatures. And vice versa. It is not possible to draw any conclusions on this relationship from the output of this research. Further investigation into this possible causal link is required. (RWS: Rather look for cases in the literature in which stable states occur during winter months that could argue for this observation.)

4.3. Spatiality

That 8 of the 9 nodes created by the SOM consist of synoptic air-sea states that occurred during MHWs on different coastal sections of the study area leads to two possible implications. (RWS: Rewrite this sentence if you don't simply remove this subsection instead.) The first is that the onshore forcing of the Agulhas current during thee MHWs must be extending onto the shore through the Benguela

upwelling system. The other implication is that it may be temperature exchange between air and sea at the coast that is leading to these events. (RWS: Must expound upon these two ideas more fully.)

4.4. Normal days

Move the above two sections here.

5. Conclusion

This research has highlighted that coastal MHWs with durations in excess of 15 days often occur during the abnormal advection of water onto the coast due to atypical meso-scale activity. In the case of the west and south coast sections of South Africa this offshore water is often warmer than coastal waters and so it was not necessary that the offshore waters be aseasonally warm at their point of origin. Anomalous wind and air temperature patterns during coastal MHWs were found to cover a wide range of states and so no one pattern shows a clear relationship to these events.

It was also found that the average synoptic air-sea states found during coastal MHWs do not relate closely to any of the normal air-sea states seen throughout the year. (RWS: Also discuss the atmospheric results.) This means that the meso-scale activity that is occurring during these MHWs is not represented by typical conditions that occur seasonally. Furthermore, the fewest MHWs occurred during summer months than any other season. These two facts taken together support the argument that MHWs are not simply a symptom of solar heating during the warm months of the year, but that other phenomena are having a more pronounced effect on the atypical warming we have documented. (RWS: Now that I think about it, if it is indeed that most MHWs are caused by Agulhas Leakage, the reason there are fewer in the summer would be that coastal temperatures are closer to the Agulhas temperature in the summer. So if there is leakage it wouldn't necessarily show up.)

The mean air-sea state during the longest, most cumulatively intense events (node 4, table 2, fig. 4) was also one of the least anomalous. Meaning that for some of the events which could have potentially had the most negative impact on nearshore ecosystems, there does not appear to be any large scale forcing from the air or sea on coastal waters during those times.

This finding shows that a knowledge of the meso-scale oceanographic and atmospheric properties of an area are necessary to determine what forces may be causing MHWs along a stretch of coastline. But that even with this knowledge, many of the largest MHWs do not show any relationship to these potential meso-scale forces. One must therefore not assume that meso-scale activity in either the air or sea may be at the root of any particularly large MHWs observed in nearshore environments. Finer spatial resolutions must be considered when investigating such events. This is however challenging as such high resolution *in situ* data are often very sparse.

It is therefore advised that areas of particular susceptibility to MHWs be identified in order to allow for finer scale monitoring of these areas to be supported. Once these areas have been identified and such monitoring systems installed, it may then be possible to better determine what leads to coastal MHWs.

(RWS: Expand on this to better match the abstract.)

Table 3: The metadata and coastal averages for all *in situ* time series used in this study.

	order	site	src	index	lon	lat	depth	type	coast	date.start	date.end	length	N
84	2	Port Nolloth	SAWS	Port Nolloth/ SAWS	16.87	-29.25	0	thermo	wc	1299.00	16800.00	15502	
100	16	Sea Point	SAWS	Sea Point/ SAWS	18.38	-33.92	0	thermo	wc	1461.00	16527.00	15067	
71	17	Oudekraal	DAFF	Oudekraal/ DAFF	18.35	-33.98	9	UTR	wc	12108.00	16835.00	4728	
41	18	Hout Bay	DEA	Hout Bay/ DEA	18.35	-34.05	28	UTR	wc	7753.00	13992.00	6240	
52	20	Kommetjie	SAWS	Kommetjie/ SAWS	18.33	-34.14	0	thermo	wc	8095.00	16527.00	8433	
12	22	Bordjies	DAFF	Bordjies/ DAFF	18.46	-34.32	4	UTR	sc	12502.00	16748.00	4247	
13	23	Bordjies Deep	DAFF	Bordjies Deep/ DAFF	18.47	-34.31	9	UTR	sc	12087.00	16748.00	4662	
33	27	Fish Hoek	SAWS	Fish Hoek/ SAWS	18.44	-34.14	0	thermo	sc	8095.00	16527.00	8433	
65	29	Muizenberg	SAWS	Muizenberg/ SAWS	18.48	-34.10	0	thermo	sc	1220.00	16527.00	15308	
36	30	Gordons Bay	SAWS	Gordons Bay/ SAWS	18.86	-34.16	0	thermo	sc	986.00	16527.00	15542	
10	31	Betty's Bay	DAFF	Betty's Bay/ DAFF	18.92	-34.36	5	UTR	sc	12765.00	16751.00	3987	
38	32	Hermanus	SAWS	Hermanus/ SAWS	19.25	-34.41	0	thermo	sc	7274.00	16527.00	9254	
109	37	Stilbaai	SAWS	Stilbaai/ SAWS	21.44	-34.37	0	thermo	sc	3652.00	16527.00	12876	
131	38	Ystervarkpunt	DEA	Ystervarkpunt/ DEA	21.74	-34.40	3	UTR	sc	9426.00	13685.00	4260	
61	39	Mossel Bay	DEA	Mossel Bay/ DEA	22.16	-34.18	8	UTR	sc	7846.00	13685.00	5840	
50	42	Knysna	DEA	Knysna/ DEA	23.07	-34.08	7	UTR	sc	9210.00	14554.00	5345	
119	45	Tsitsikamma West	SAWS	Tsitsikamma/ SAWS	23.65	-33.98	0	thermo	sc	7486.00	13559.00	6074	
111	46	Storms River Mouth	SAWS	Storms River Mouth/ SAWS	23.90	-34.02	0	thermo	sc	8491.00	14244.00	5754	
118	47	Tsitsikamma East	DEA	Tsitsikamma/ DEA	23.91	-34.03	10	UTR	sc	7849.00	14558.00	6710	
78	58	Pollock Beach	SAWS	Pollock Beach/ SAWS	25.68	-33.99	0	thermo	sc	10724.00	16527.00	5804	
43	59	Humewood	SAWS	Humewood/ SAWS	25.65	-33.97	0	thermo	sc	1332.00	10956.00	9625	
37	67	Hamburg	DEA	Hamburg/ DEA	27.49	-33.29	4	UTR	sc	9433.00	14667.00	5235	
30	68	Eastern Beach	SAWS	Eastern Beach/ SAWS	27.92	-33.02	0	thermo	ec	5113.00	10438.00	5326	
70	69	Orient Beach	SAWS	Orient Beach/ SAWS	27.92	-33.02	0	thermo	ec	5113.00	16527.00	11415	
68	70	Nahoon Beach	SAWS	Nahoon Beach/ SAWS	27.95	-32.99	0	thermo	ec	5113.00	10438.00	5326	
102	133	Sodwana	DEA	Sodwana/ DEA	32.73	-27.42	18	UTR	ec	8835.00	14636.00	5802	

Acknowledgements

We would like to thank DAFF, DEA, EKZNW, KZNSB, SAWS and SAEON for contributing all of the raw data used in this study. Without it, this article and the South African Coastal Temperature Network (SACTN) would not be possible. We would also like to thank Dr. Andries Kruger for his contributions to this work. This research was supported by NRF Grant (CPRR14072378735). This paper makes a contribution to the objectives of the Australian Research Council Centre of Excellence for Climate System Science (ARCCSS). The authors report no financial conflicts of interests. The data and analyses used in this paper may be found at https://github.com/schrob040/MHW. The Bluelink ocean data products were provided by CSIRO. Bluelink is a collaboration involving the Commonwealth Bureau of Meteorology, the Commonwealth Scientific and Industrial Research Organisation and the Royal Australian Navy.

Supplementary

Meta-data

Further meta-data for each time series and source listed in geographic order along the South African coast from the border of Namibia to the border of Mozambique may be found in Table 3.

References

Barrett, J. E., Virginia, R. A., Wall, D. H., Doran, P. T., Fountain, A. G., Welch, K. A., Lyons, W. B., oct 2008. Persistent effects of a discrete warming event on a polar desert ecosystem. Global Change

Biology 14 (10), 2249–2261.
URL http://doi.wiley.com/10.1111/j.1365-2486.2008.01641.x

Beal, L. M., De Ruijter, W. P. M., Biastoch, A., Zahn, R., Cronin, M., Hermes, J., Lutjeharms, J., Quartly, G., Tozuka, T., Baker-Yeboah, S., Bornman, T., Cipollini, P., Dijkstra, H., Hall, I., Park, W., Peeters, F., Penven, P., Ridderinkhof, H., Zinke, J., 2011. On the role of the Agulhas system in ocean circulation and climate. Nature 472 (7344), 429–436.
URL http://www.nature.com/doifinder/10.1038/nature09983

Benthuysen, J., Feng, M., Zhong, L., 2014. Spatial patterns of warming off Western Australia during the 2011 Ningaloo Niño: quantifying impacts of remote and local forcing. Continental Shelf Research 91, 232–246.

Blamey, L. K., Shannon, L. J., Bolton, J. J., Crawford, R. J., Dufois, F., Evers-King, H., Griffiths, C. L., Hutchings, L., Jarre, A., Rouault, M., Watermeyer, K. E., Winker, H., apr 2015. Ecosystem change in the southern Benguela and the underlying processes. Journal of Marine Systems 144, 9–29.
URL http://linkinghub.elsevier.com/retrieve/pii/S092479631400311X

Bond, N. A., Cronin, M. F., Freeland, H., Mantua, N., may 2015. Causes and impacts of the 2014 warm anomaly in the NE Pacific. Geophysical Research Letters 42 (9), 3414–3420.
URL http://doi.wiley.com/10.1002/2015GL063306

Boucek, R. E., Gaiser, E. E., Liu, H., Rehage, J. S., oct 2016. A review of subtropical community resistance and resilience to extreme cold spells. Ecosphere 7 (10), e01455.
URL http://doi.wiley.com/10.1002/ecs2.1455

Burrough, P. A., Wilson, J. P., Van Gaans, P. F. M., Hansen, A. J., 2001. Fuzzy k-means classification of topo-climatic data as an aid to forest mapping in the Greater Yellowstone Area, USA. Landscape Ecology 16 (6), 523–546.

Burrows, M. T., Schoeman, D. S., Buckley, L. B., Moore, P., Poloczanska, E. S., Brander, K. M., Brown, C., Bruno, J. F., Duarte, C. M., Halpern, B. S., Holding, J., Kappel, C. V., Kiessling, W., O'Connor, M. I., Pandolfi, J. M., Parmesan, C., Schwing, F. B., Sydeman, W. J., Richardson, A. J., nov 2011. The pace of shifting climate in marine and terrestrial ecosystems. Science 334 (6056), 652–655.
URL http://www.sciencemag.org/cgi/doi/10.1126/science.1210288http://www.sciencemag.org/content/334/6056/652.abstract{%}5Cnhttp://www.sciencemag.org/content/334/6056/652.full.pdf

Castillo, K. D., Lima, F. P., 2010. Comparison of in situ and satellite-derived (MODIS-Aqua/Terra) methods for assessing temperatures on coral reefs. Limnology and Oceanography Methods 8, 107–117.

Cavazos, T., 2000. Using self-organizing maps to investigate extreme climate events: An application to wintertime precipitation in the Balkans. Journal of Climate 13 (10), 1718–1732.

Cavole, L., Demko, A., Diner, R., Giddings, A., Koester, I., Pagniello, C., Paulsen, M.-L., Ramirez-Valdez, A., Schwenck, S., Yen, N., Zill, M., Franks, P., 2016. Biological Impacts of the 2013–2015 Warm-Water Anomaly in the Northeast Pacific: Winners, Losers, and the Future. Oceanography 29 (2).
URL https://tos.org/oceanography/article/biological-impacts-of-the-20132015-warm-water-anomaly-i

Chen, K., Gawarkiewicz, G., Kwon, Y.-O., Zhang, W. G., jun 2015. The role of atmospheric forcing versus ocean advection during the extreme warming of the Northeast U.S. continental shelf in 2012. Journal of Geophysical Research: Oceans 120 (6), 4324–4339.
URL http://doi.wiley.com/10.1002/2014JC010547

Corte-Real, J., Qian, B., Xu, H., 1998. Regional climate change in Portugal: precipitation variability associated with large-scale atmospheric circulation. International Journal of Climatology 18 (6), 619–635.
URL http://onlinelibrary.wiley.com/doi/10.1002/(SICI)1097-0088(199805)18:6{%}3C619::AID-JOC271{%}3E3.0.CO;2-T/abstracthttp://www.scopus.com/scopus/inward/record.url?eid=2-s2.0-3543007704{&}partnerID=40{&}rel=R7.0.0

Cox, P. M., Betts, R. a., Jones, C. D., Spall, S. a., Totterdell, I. J., 2000. Acceleration of global warming due to carbon-cycle feedbacks in a coupled climate model. Nature 408 (6809), 184–187.

Dee, D. P., Uppala, S. M., Simmons, A. J., Berrisford, P., Poli, P., Kobayashi, S., Andrae, U., Balmaseda, M. A., Balsamo, G., Bauer, P., Bechtold, P., Beljaars, A. C. M., van de Berg, L., Bidlot, J., Bormann, N., Delsol, C., Dragani, R., Fuentes, M., Geer, A. J., Haimberger, L., Healy, S. B., Hersbach, H., Hólm, E. V., Isaksen, L., Kållberg, P., Köhler, M., Matricardi, M., McNally, A. P., Monge-Sanz, B. M., Morcrette, J.-J., Park, B.-K., Peubey, C., de Rosnay, P., Tavolato, C., Thépaut, J.-N., Vitart, F., apr 2011. The ERA-Interim reanalysis: configuration and performance of the data assimilation system. Quarterly Journal of the Royal Meteorological Society 137 (656), 553–597.
URL http://doi.wiley.com/10.1002/qj.828

Denny, M. W., Hunt, L. J. H., Miller, L. P., Harley, C. D. G., aug 2009. On the prediction of extreme ecological events. Ecological Monographs 79 (3), 397–421.
URL http://doi.wiley.com/10.1890/08-0579.1

Easterling, D. R., Meehl, G. A., Parmesan, C., Changnon, S. A., Karl, T. R., Mearns, L. O., 2000. Climate extremes: observations, modeling, and impacts. Science 289 (5487), 2068–2074.

Feng, M., McPhaden, M. J., Xie, S.-P., Hafner, J., 2013. La Niña forces unprecedented Leeuwin Current warming in 2011. Scientific Reports 3, 1277.

Garrabou, J., Coma, R., Bensoussan, N., Bally, M., Chevaldonné, P., Cigliano, M., Diaz, D., Harmelin, J. G., Gambi, M. C., Kersting, D. K., Ledoux, J. B., Lejeusne, C., Linares, C., Marschal, C., Pérez, T., Ribes, M., Romano, J. C., Serrano, E., Teixido, N., Torrents, O., Zabala, M., Zuberer, F., Cerrano,

C., 2009. Mass mortality in Northwestern Mediterranean rocky benthic communities: effects of the 2003 heat wave. Global Change Biology 15 (5), 1090–1103.

GORDON, G., BROWN, A. S., PULSFORD, T., dec 1988. A koala (Phascolarctos cinereus Goldfuss) population crash during drought and heatwave conditions in south-western Queensland. Austral Ecology 13 (4), 451–461.
URL http://doi.wiley.com/10.1111/j.1442-9993.1988.tb00993.x

Grebmeier, J. M., mar 2006. A Major Ecosystem Shift in the Northern Bering Sea. Science 311 (5766), 1461–1464.
URL http://www.sciencemag.org/cgi/doi/10.1126/science.1121365

Gunter, G., 1941. Death of fishes due to cold on the Texas coast, January, 1940. Ecology 22 (2), 203–208.

Hansen, J., Johnson, D., Lacis, A., Lebedeff, S., Lee, P., Rind, D., Russell, G., 1981. Climate Impact of Increasing Atmospheric Carbon Dioxide. Science 213 (4511), 957–966.
URL http://www.sciencemag.org/cgi/doi/10.1126/science.213.4511.957

Hewitson, B. C., Crane, R. G., 2002. Self-organizing maps: Applications to synoptic climatology. Climate Research 22 (1), 13–26.

Hobday, A. J., Alexander, L. V., Perkins, S. E., Smale, D. A., Straub, S. C., Oliver, E. C., Benthuysen, J. A., Burrows, M. T., Donat, M. G., Feng, M., Holbrook, N. J., Moore, P. J., Scannell, H. A., Sen Gupta, A., Wernberg, T., 2016. A hierarchical approach to defining marine heatwaves. Progress in Oceanography 141, 227–238.

Hufkens, K., Friedl, M. A., Keenan, T. F., Sonnentag, O., Bailey, A., O'Keefe, J., Richardson, A. D., jul 2012. Ecological impacts of a widespread frost event following early spring leaf-out. Global Change Biology 18 (7), 2365–2377.
URL http://doi.wiley.com/10.1111/j.1365-2486.2012.02712.x

Hutchings, L., van der Lingen, C. D., Shannon, L. J., Crawford, R. J. M., Verheye, H. M. S., Bartholomae, C. H., van der Plas, a. K., Louw, D., Kreiner, A., Ostrowski, M., Fidel, Q., Barlow, R. G., Lamont, T., Coetzee, J., Shillington, F., Veitch, J., Currie, J. C., Monteiro, P. M. S., 2009. The Benguela Current: an ecosystem of four components. Progress in Oceanography 83 (1-4), 15–32.

Jain, A. K., 2010. Data clustering: 50 years beyond K-means. Pattern Recognition Letters 31 (8), 651–666.

Johnson, N. C., 2013. How many enso flavors can we distinguish? Journal of Climate 26 (13), 4816–4827.

Jolly, W. M., Dobbertin, M., Zimmermann, N. E., Reichstein, M., sep 2005. Divergent vegetation growth responses to the 2003 heat wave in the Swiss Alps. Geophysical Research Letters 32 (18),

n/a–n/a.
URL http://doi.wiley.com/10.1029/2005GL023252

Kumar, J., Mills, R. T., Hoffman, F. M., Hargrove, W. W., 2011. Parallel k-means clustering for quantitative ecoregion delineation using large data sets. In: Procedia Computer Science. Vol. 4. pp. 1602–1611.

Lirman, D., Schopmeyer, S., Manzello, D., Gramer, L. J., Precht, W. F., Muller-Karger, F., Banks, K., Barnes, B., Bartels, E., Bourque, A., Byrne, J., Donahue, S., Duquesnel, J., Fisher, L., Gilliam, D., Hendee, J., Johnson, M., Maxwell, K., McDevitt, E., Monty, J., Rueda, D., Ruzicka, R., Thanner, S., 2011. Severe 2010 cold-water event caused unprecedented mortality to corals of the Florida reef tract and reversed previous survivorship patterns. PLOS ONE 6 (8).

Lünning, K., 1990. Seaweds: their environment, biogeography and ecophysiology. John Wiley and Sons. Wiley, New York (USA).

Lutjeharms, J., Cooper, J., Roberts, M., apr 2000. Upwelling at the inshore edge of the Agulhas Current. Continental Shelf Research 20 (7), 737–761.
URL http://linkinghub.elsevier.com/retrieve/pii/S0278434399000928

Manabe, S., Wetherald, R. T., 1967. Thermal Equilibrium of the Atmosphere with a Given Distribution of Relative Humidity. Journal of the Atmospheric Sciences 24 (3), 241–259.
URL http://journals.ametsoc.org/doi/abs/10.1175/1520-0469{%}281967{%}29024{%}3C0241{%}3ATEOTAW{%}2.0.CO{%}3B2

Mills, K., Pershing, A., Brown, C., Chen, Y., Chiang, F.-S., Holland, D., Lehuta, S., Nye, J., Sun, J., Thomas, A., Wahle, R., 2013. Fisheries Management in a Changing Climate: Lessons From the 2012 Ocean Heat Wave in the Northwest Atlantic. Oceanography 26 (2).
URL https://tos.org/oceanography/article/fisheries-management-in-a-changing-climate-lessonsfrom-

Morioka, Y., Tozuka, T., Yamagata, T., 2010. Climate variability in the southern Indian Ocean as revealed by self-organizing maps. Climate Dynamics 35 (6), 1075–1088.

Pearce, A. F., Feng, M., 2013. The rise and fall of the "marine heat wave" off Western Australia during the summer of 2010/2011. Journal of Marine Systems 111-112, 139–156.

Perkins, S. E., Alexander, L. V., 2013. On the measurement of heat waves. Journal of Climate 26 (13), 4500–4517.

Perkins-Kirkpatrick, S. E., White, C. J., Alexander, L. V., Argüeso, D., Boschat, G., Cowan, T., Evans, J. P., Ekström, M., Oliver, E. C., Phatak, A., Purich, A., 2016. Natural hazards in Australia: heatwaves. Climatic Change 139 (1), 101–114.

Rosenzweig, C., Karoly, D., Vicarelli, M., Neofotis, P., Wu, Q., Casassa, G., Menzel, A., Root, T. L., Estrella, N., Seguin, B., Tryjanowski, P., Liu, C., Rawlins, S., Imeson, A., 2008. Attributing physical

and biological impacts to anthropogenic climate change. Nature 453 (7193), 353–357.
URL http://www.nature.com/doifinder/10.1038/nature06937

Sawyer, J. S., 1972. Man-made Carbon Dioxide and the "Greenhouse" Effect. Nature 239 (5366), 23–26.
URL http://www.nature.com/doifinder/10.1038/239023a0

Scavia, D., Field, J. C., Boesch, D. F., Buddemeier, R. W., Burkett, V., Cayan, D. R., Fogarty, M., Harwell, M. A., Howarth, R. W., Mason, C., Reed, D. J., Royer, T. C., Sallenger, A. H., Titus, J. G., apr 2002. Climate change impacts on U.S. Coastal and Marine Ecosystems. Estuaries 25 (2), 149–164.
URL http://link.springer.com/10.1007/BF02691304

Schaeffer, A., Roughan, M., 2017. Sub-surface intensification of marine heatwaves off southeastern Australia: the role of stratification and local winds. Geophysical Research Letters.
URL http://doi.wiley.com/10.1002/2017GL073714

Schlegel, R. W., Oliver, E. C. J., Wernberg, T., Smit, A. J., 2017. Nearshore and offshore co-occurrence of marine heatwaves and cold-spells. Progress in Oceanography 151, 189–205.
URL http://dx.doi.org/10.1016/j.pocean.2017.01.004

Schlegel, R. W., Smit, A. J., 2016. Climate Change in Coastal Waters: Time Series Properties Affecting Trend Estimation. Journal of Climate 29 (24), 9113–9124.
URL http://journals.ametsoc.org/doi/10.1175/JCLI-D-16-0014.1

Smale, D. A., Wernberg, T., 2009. Satellite-derived SST data as a proxy for water temperature in nearshore benthic ecology Peer reviewed article. Marine Biology 387, 27–37.

Smit, A. J., Roberts, M., Anderson, R. J., Dufois, F., Dudley, S. F. J., Bornman, T. G., Olbers, J., Bolton, J. J., 2013. A coastal seawater temperature dataset for biogeographical studies: large biases between in situ and remotely-sensed data sets around the coast of South Africa. PLOS ONE 8 (12).

Stachowicz, J. J., Terwin, J. R., Whitlatch, R. B., Osman, R. W., nov 2002. Linking climate change and biological invasions: Ocean warming facilitates nonindigenous species invasions. Proceedings of the National Academy of Sciences 99 (24), 15497–15500.
URL http://www.pnas.org/cgi/doi/10.1073/pnas.242437499

Stocker, T., Qin, D., Plattner, G. K., Tignor, M., Allen, S. K., Boschung, J., Nauels, A., Xia, Y., Bex, V., Midgley, P. M. (Eds.), 2013. Climate change 2013: the physical science basis: Working Group I contribution to the Fifth Assessment Report of the Intergovernmental Panel on Climate Change. Cambridge University Press, Cambridge, United Kingdom and New York, NY, USA.

Stott, P. A., Stone, D. A., Allen, M. R., dec 2004. Human contribution to the European heatwave of 2003. Nature 432 (7017), 610–614.
URL http://www.nature.com/doifinder/10.1038/nature03089

Thomas, C. D., Cameron, A., Green, R. E., Bakkenes, M., Beaumont, L. J., Collingham, Y. C., Erasmus, B. F. N., de Siqueira, M. F., Grainger, A., Hannah, L., Hughes, L., Huntley, B., van Jaarsveld, A. S., Midgley, G. F., Miles, L., Ortega-Huerta, M. A., Townsend Peterson, A., Phillips, O. L., Williams, S. E., 2004. Extinction risk from climate change. Nature 427 (6970), 145–148.
URL http://www.nature.com/doifinder/10.1038/nature02121

Travis, J. M. J., 2003. Climate change and habitat destruction: a deadly anthropogenic cocktail. Proceedings of the Royal Society B: Biological Sciences 270 (1514), 467–473.
URL http://rspb.royalsocietypublishing.org/cgi/doi/10.1098/rspb.2002.2246

Unal, Y., Kindap, T., Karaca, M., 2003. Redefining the climate zones of Turkey using cluster analysis. International Journal of Climatology 23 (9), 1045–1055.

Walther, G.-R., Post, E., Convey, P., Menzel, A., Parmesan, C., Beebee, T. J. C., Fromentin, J.-M., Hoegh-Guldberg, O., Bairlein, F., mar 2002. Ecological responses to recent climate change. Nature 416 (6879), 389–395.
URL http://www.nature.com/doifinder/10.1038/416389a

Wernberg, T., Bennett, S., Babcock, R. C., Bettignies, T. D., Cure, K., Depczynski, M., Dufois, F., Fromont, J., Fulton, C. J., Hovey, R. K., Harvey, E. S., Holmes, T. H., Kendrick, G. A., Radford, B., Santana-garcon, J., Saunders, B. J., Smale, D. A., Thomsen, M. S., 2016. Climate driven regime shift of a temperate marine ecosystem. Science 149 (1996), 2009–2012.

Wernberg, T., Russell, B. D., Moore, P. J., Ling, S. D., Smale, D. A., Campbell, A., Coleman, M. A., Steinberg, P. D., Kendrick, G. A., Connell, S. D., 2011. Impacts of climate change in a global hotspot for temperate marine biodiversity and ocean warming. Journal of Experimental Marine Biology and Ecology 400 (1-2), 7–16.

Wernberg, T., Smale, D. a., Tuya, F., Thomsen, M. S., Langlois, T. J., de Bettignies, T., Bennett, S., Rousseaux, C. S., 2012. An extreme climatic event alters marine ecosystem structure in a global biodiversity hotspot. Nature Climate Change 3 (8), 78–82.
URL http://www.nature.com/doifinder/10.1038/nclimate1627